

AUTOMATIC SLEEP STAGE CLASSIFICATION USING MULTI-PHYSIOLOGICAL SIGNALS BASED ON PCBSLEEPNET

YuLi Yang, Ying Liu, HaoWei Zhang*

School of Health Science and Engineering, University of Shanghai for Science and Technology, Shanghai 200093, China.

**Corresponding Author: HaoWei Zhang*

Abstract: Automatic sleep staging, a key technology in sleep medicine, faces feature selection challenges due to multi-modal physiological signal heterogeneity. This study establishes a framework to evaluate bioelectrical signals' impacts on deep neural network feature representation, aiming to identify optimal integration paradigms. We propose a multi-branch hybrid neural network with: 1) a three-channel parallel convolutional module incorporating cascaded residual and dilated convolutions for time-frequency feature extraction, and 2) bidirectional long short-term memory (BiLSTM) layers for temporal dependency modeling. We systematically analyzed multi-channel electroencephalogram (EEG), single-channel physiological signals, and their combinations covering both single-channel and multi-channel configurations of EEG, electrooculogram (EOG), and electromyogram (EMG). Results demonstrate that six-channel EEG configurations outperformed single/dual-channel implementations. In the single- and dual-channel EEG settings, the C3-M2 and C4-M1 + C3-M2 channels exhibited superior performance. EEG maintained superior classification capability over EOG/EMG. The tri-modal fusion (EEG+EOG+EMG) achieved peak performance (accuracy: 89.5%, Cohen's κ : 0.85). This demonstrates EEG's central role in sleep staging, while EOG/EMG synergistically enhance model performance. The findings reveal heterogeneous bioelectric signal interactions in deep neural networks, providing foundations for optimizing signal fusion strategies and model architectures.

Keywords: Deep learning; Sleep staging; Multi-physiological signals; Polysomnography

1 INTRODUCTION

Sleep accounts for one-third of life, and good sleep is vital for metabolism and immune regulation[1-2]. About 33% of the global population experiences sleep issues[3]. Thus, evaluating sleep quality and diagnosing disorders is essential[4]. Clinically, polysomnography (PSG) is commonly used to collect and record physiological signals such as electroencephalogram (EEG), electrooculogram (EOG), and electromyogram (EMG) from patients throughout the night[5]. PSG recordings last about 8 hours. Experts use the sleep scoring standards provided by the American Academy of Sleep Medicine (AASM) [6]. Signals are labeled per 30-second epochs[7]. This process visually examines spindle waves and frequency features to classify sleep stages[8-9]. Manual sleep stage labeling is error-prone and time-consuming[10-11], and it consumes significant amounts of time, money, and human resources[12].

Early research on sleep stage classification methods primarily focused on using EEG signals as input[13-15], achieving relatively high accuracy, but single-channel EEG lacks sufficient information[16]. Experts still need to consider other physiological signals when manually labeling sleep stages. In recent years, some researchers have focused on the multichannel domain[17-18]. However, most studies have used machine learning combined with multi-channel physiological signals. This method depends on manual features. With the development of artificial intelligence and computer technology, deep learning has gradually been applied to the field of biosignal processing[19-20]. Although many solutions have been designed for the automated classification of sleep stages, no system has yet fully replaced human experts as the gold standard[21]. One reason for this is that the physiological signals used are not comprehensive enough, making it difficult to promote these models in clinical settings.

Based on the previously proposed automatic sleep stage classification model (PreData-CNN-BiLSTM-SleepNet, PCBSleepNet) that uses a single-channel EEG signal combined with a deep convolutional neural network (DCNN) and bidirectional long short-term memory network (BiLSTM)[22], this study further investigates the automatic sleep staging using PSG-recorded multi-physiological signals, selecting multi-channel EEG signals, other single-channel physiological signals, and mixed physiological signals as model inputs. The aim is to study the impact of different input signals on the performance of the automatic sleep staging model and to explore the intrinsic relationships between various physiological signals and sleep stages.

2 MATERIALS AND METHODS

This study utilizes PCBSleepNet from prior work[22]. The model has three parallel CNN layers with different kernel sizes for time-frequency feature extraction. Dilated CNNs accelerate feature fusion, while three BiLSTM layers capture bidirectional temporal dependencies. The model uses Softmax for classification. Figure 1 presents the experimental process. Sleep monitoring was conducted at Shanghai Mental Health Center using the PSG-1100 system. Physiological signals were recorded overnight. Data preprocessing included signal denoising and

augmentation. The processed data were input into a deep CNN for feature extraction and fusion. A sequential network captured temporal features. Extracted features were classified, and the model was optimized iteratively for sleep staging.

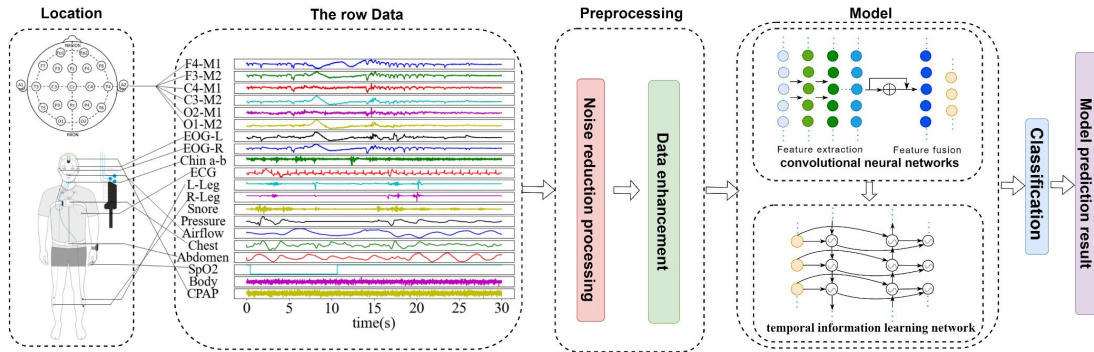


Figure 1 Experimental Workflow Diagram

2.1 Experimental Dataset

This study used the Shanghai Mental Health Center Sleep Database (SMHCSD), which contains 148 full-night PSG recordings and associated medical diagnostic reports. Each PSG recording includes six dual-channel EEGs, two EOGs, EMG, airflow, ECG, and other physiological data. Sleep staging follows AASM standards, mainly analyzing EEG (brain waves), EOG (eye movement), and EMG (muscle tone)[6]. These three signals provide core data for sleep staging. Thus, this study focuses on EEG, EOG, and EMG for automatic sleep staging. All signals are sampled at 200 Hz. SMHCSD provides AASM-labeled sleep stages: Wake (W), N1, N2, N3, REM, MOVEMENT, UNKNOWN. MOVEMENT marks nighttime activity; UNKNOWN indicates undetermined frames, treated as invalid. The study meets AASM 2.4 criteria and is approved by the Ethics Committee (No. 2020-23).

2.2 Data Preprocessing

After collecting the raw PSG signals, the first step is data cleaning, which involves removing invalid sleep stage data, such as MOVEMENT and UNKNOWN stages. Next, preprocessing is performed on the EEG, EOG, and EMG signals required for the study.

2.2.1 Noise reduction

Signals often suffer from interference, including subject movements and external noise, causing contamination. Thus, preprocessing enhances data quality. It includes noise removal, normalization, and data augmentation. WPD, an orthogonal decomposition method, analyzes signals across all frequencies, providing finer analysis than traditional wavelet denoising[23], offering more refined signal analysis compared to traditional wavelet denoising. WPD improves frequency resolution across low- and high-frequency bands by multi-level decomposition. For complex signals, this method distinguishes noise at different levels, aiding denoising. Figure 2(a) illustrates the three-level WPD denoising structure.

packet coefficient at position p of level j be $d_j^p(k)$. The corresponding wavelet packet decomposition coefficients at level $j+1$ are defined by Equations (1) and (2):

$$d_{j+1}^{2p}(k) = \sum_m d_j^p(m)h(m-2k) \quad (1)$$

$$d_{j+1}^{2p+1}(k) = \sum_m d_j^p(m)g(m-2k) \quad (2)$$

In the above equations, $h(k)$ represents the low-pass filter, and $g(k)$ represents the high-pass filter. The wavelet packet coefficient at position (j,p) is d_j^p , and the reconstruction formula is shown as Equation (3):

$$d_j^p(k) = \sum_m \left[d_{j+1}^{2p}(m)h(k-2m) + d_{j+1}^{2p+1}(m)g(k-2m) \right] \quad (3)$$

Four Daubechies and two Coiflet wavelet basis functions decomposed signals at levels 3 to 6. Signal-to-noise ratio (SNR) and mean square error (MSE) were employed as evaluation metrics to select the optimal wavelet basis function and decomposition level. A random sample was used for verification, with the same method applied to all data. Figure 2(b) presents an EEG frame analysis from this sample. Thus, the db10 wavelet function was used to denoise EEG, EOG, and EMG signals. Figure 2(c) compares signals before and after denoising. After WPD, noise was significantly reduced, improving signal quality.

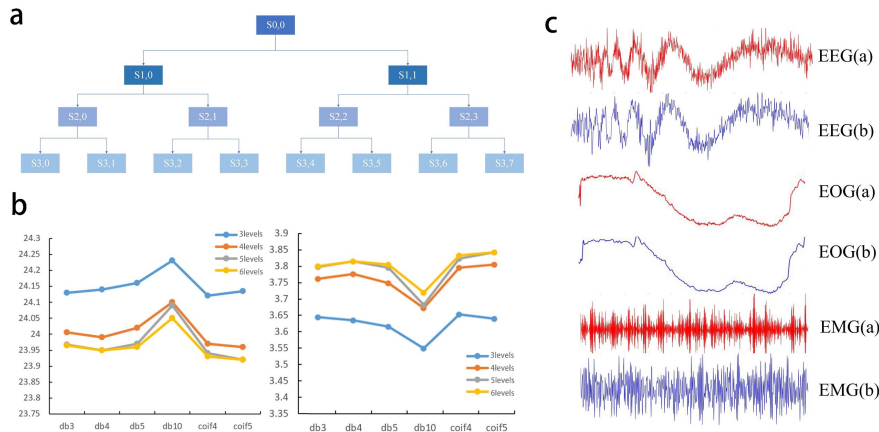


Figure 2 Data Preprocessing: a. Three-level WPD Decomposition Structure: The Diagram Illustrates a Three-Level Decomposition of Input Signal S . The Left Section Shows Low-Frequency Decomposition, While the Right Represents High-Frequency Decomposition. b. Denoising Parameter Variation after 3 to 6 Decomposition Levels: Left—SNR; Right—MSE. c. Comparison of Signals before and after WPD: (a) Original Signal, (b) Denoised Signal.

2.2.2 Data augmentation

As per AASM standards, full-night EEG, EOG, and EMG signals were segmented into 30-second epochs. Each subject's signals yielded about 1,000 frames. Epochs were matched with expert-annotated sleep stage labels. Table 1 presents the epoch distribution for each sleep stage in the SMHCSD dataset. Table 1 shows a significant variation in epoch distribution across sleep stages, highlighting a class imbalance issue. To address this issue, the Adaptive Synthetic Sampling (ADASYN) technique was applied to optimize the dataset[24]. The key advantage of ADASYN is its ability to automatically determine the number of synthetic samples needed for the minority class based on the overall sample distribution, thereby balancing the dataset, as illustrated in Figure 3.

Table 1 Number of Sample Epochs in Each Sleep Stage

Dataset	W	N1	N2	N3	REM	Total
SMHCSD	34904	16616	70065	6587	15223	143395

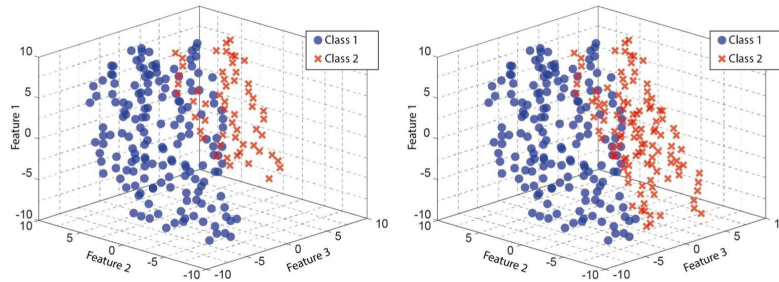


Figure 3 Data Augmentation Using ADASYN (a) Sample Distribution of Raw Data; (b) Sample Distribution after ADASYN Enhancement

2.3 Model Design

2.3.1 Feature extraction module

The feature extraction module employs three parallel 1D-CNNs with kernel sizes of 3, 5, and 7, as illustrated in Figure 4(a). Each branch consists of four convolutional layers and an adaptive average pooling layer (AdaptiveAvgPool1d). To counteract performance degradation from deep networks, residual connections were added between every two convolutional layers. The mapping function was defined by a ReLU activation function. Each convolutional layer is characterized by its kernel size, channel dimensions, and stride. Based on the experimental setup detailed[22], the network structure was adjusted according to the number of input signal channels. The features extracted by the three parallel networks are concatenated to form the output vector $F \in R^{N \times 1}$, where N represents the length of the feature vector. This output is then passed to the feature fusion module. The one-dimensional convolution operation within the convolutional layers is represented by Equation(4)

$$y_i^l = \phi \left[g_p \left(\sum_{n=1}^d w_n^l \cdot y_i^{l-1} + b^l \right) \right], \quad i \in (1, N - d + 1) \quad (4)$$

In the above equation: y_i^l represents the i -th feature vector in the output feature set of the l -th layer; y_i^{l-1} denotes the i -th feature vector from the output of the previous layer; ϕ represents the activation function; g_{p^l} denotes the down-sampling operation with a stride of p^l ; w^l represents the weight vector; b^l indicates the bias vector; and d refers to the size of the convolutional kernel.

2.3.2 Feature fusion model

The feature fusion module comprises three dilated convolution layers, each with increasing dilation rates of 1, 2, and 4. Assuming the dilation rate is represented by the variable d , the actual convolution kernel size after applying dilation is represented in Equations (5) and (6)

$$K_h = k_h + (k_h - 1) \cdot (d - 1) \quad (5)$$

$$K_w = k_w + (k_w - 1) \cdot (d - 1) \quad (6)$$

where K_h and K_w represent the height and width of the dilated convolution kernel, while k_h and k_w represent the original kernel dimensions. The feature vector $F \in R^{N \times 1}$ output by the feature extraction module serves as the input to the feature fusion module, while $G \in R^{N \times 1}$ represents the output feature vector resulting from the feature fusion module.

2.3.3 Temporal information learning network

Physiological bioelectrical signals are highly random, nonlinear time-series data[25], encompassing both time-frequency and temporal features. The temporal learning network in this study comprises three BiLSTM layers. Each BiLSTM layer consists of a Forward LSTM (FLSTM) and a Backward LSTM (BLSTM). This structure enhances the model's ability to capture contextual information. Figure 4(c) illustrates the BiLSTM structure.

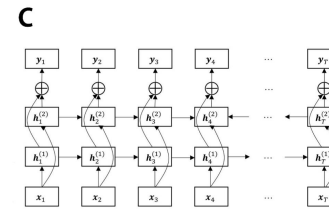
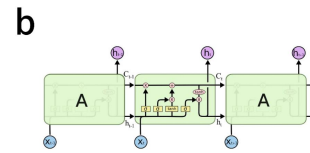
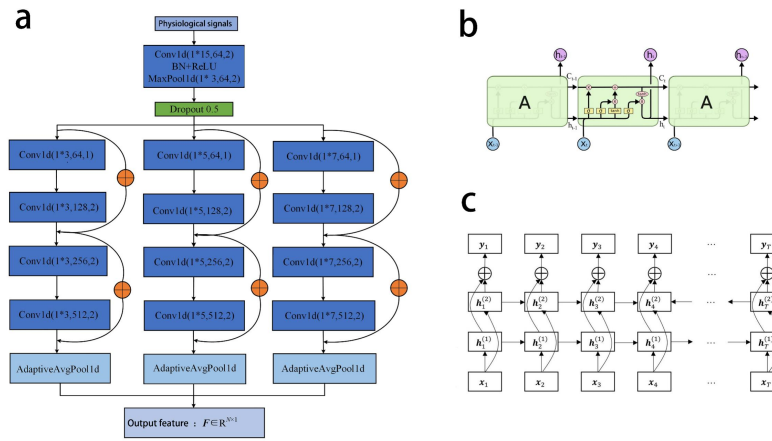


Figure 4 Model Design: (a)Feature Extraction Network Diagram; (b)LSTM Architecture; (c) BiLSTM Architecture

The principle of each propagation layer in BiLSTM is identical to that of LSTM. At the same moment, the FLSTM sequentially processes $G \in R^{N \times 1}$ to obtain the forward output $H_F \in R^{N \times 1}$, and the BLSTM sequentially processes the reversed $G \in R^{N \times 1}$ to obtain the backward output $H_B \in R^{N \times 1}$. These outputs are concatenated to form the final vector $H \in R^{N \times 1}$. This concatenated output is passed through a fully connected layer to the classification network for final sleep stage predictions. The BiLSTM equations are given in Equations (7-9).

$$h_t^{(1)} = f(U^{(1)}h_{t-1}^{(1)} + W^{(1)}x_t + b^{(1)}) \quad (7)$$

$$h_t^{(2)} = f(U^{(2)}h_{t+1}^{(2)} + W^{(2)}x_t + b^{(2)}) \quad (8)$$

$$h_t = h_t^{(1)} \oplus h_t^{(2)} \quad (9)$$

where $h_t^{(1)}$ and $h_t^{(2)}$ represent the forward and backward layer outputs, h_t represents the output result of the BiLSTM; W represents the state-input weight matrix; U represents the state-state weight matrix; and b represents the bias.

2.3.4 Classification network

The classification network uses a Softmax function to convert the multi-class output into a probability distribution over the range $[0, 1]$, selecting the class with the highest probability as the final output. The Softmax function is given by Equation (10):

$$\text{Softmax}(z_i) = \frac{e^{z_i}}{\sum_{c=1}^C e^{z_c}} \quad (10)$$

where z_i represents the output of the i -th node, and C is the total number of output classes, which corresponds to the classification labels of the samples.

2.4 Evaluation Metrics

To evaluate the performance of the proposed model, the following metrics were used: Overall Accuracy (Acc), Cohen's Kappa (Kappa), Precision (PR), Recall (RE), Micro F1-score (Micro-F1), and Macro F1-score (Macro-F1).

3 RESULTS

3.1 Results of Multichannel EEG Signal Research

The SMHCSD dataset in this study contains six dual-channel EEG signals. The signals vary depending on electrode placement. The C3-M2 channel captures electrical activity in the central and temporal regions of the left hemisphere, offering crucial information for sleep staging. F3 and F4 cover the left and right frontal lobes, respectively, playing key roles in attention, cognition, and emotional regulation. C3 and C4 cover the central regions of the left and right hemispheres, primarily involved in motor control and sensory processing. O1 and O2 cover the left and right occipital lobes, which process visual information. Figure 5(a) displays a frame of EEG waveforms from six channels. EEG signals from nearby electrodes show similarities, while those from different regions exhibit distinct patterns. Various EEG channel combinations from the preprocessed SMHCSD dataset were tested for sleep stage classification. Table 2 compares these results with previous single-channel C3-M2 scores [26]. Compared to single-channel C3-M2 EEG, C4-M1+C3-M2 and six-channel EEG combinations enhance model performance. The O2-M1+O1-M2 combination yielded relatively poor performance. The six-channel EEG configuration achieved the best performance: 89.4% accuracy, a Kappa coefficient of 0.85, and an MF1 score of 85.2%.

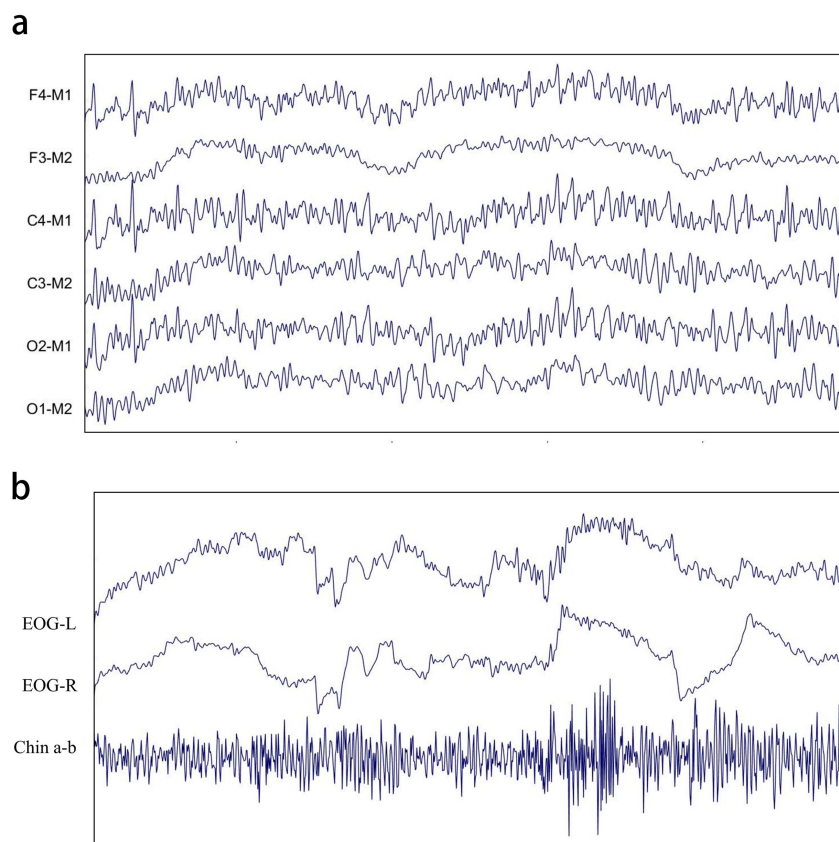


Figure 5 Forms of Signals: (a) Waveforms of EEG Signals in a Epoch of PSG Data; (b) Variations in Different Physiological Signals

Table 2 Experimental Results of Automatic Sleep Stage Modeling Using EEG Channels

EEG channels	Acc (%)	Kappa	MF1 (%)
C3-M2	88.9	0.83	84.9
F4-M1+F3-M2	88.1	0.81	83.3
C4-M1+C3-M2	89.2	0.84	85.0
O2-M1+O1-M2	81.7	0.75	75.6
six-channel EEG	89.4	0.85	85.2

3.2 Different Physiological Signals

In addition to the six EEG channels mentioned earlier, the SMHCSD dataset also includes two EOG signals (EOG-L and EOG-R) and one EMG signal (Chin a-b). These physiological signals also reflect sleep stage transitions, as

shown in Figure 5(b) It can served that the waveform fluctuations of the EOG-L signal are more pronounced compared to the EOG-R signal. The EMG signal exhibits more frequent and intense fluctuations; however, for most of the time, its waveform remains at a consistent baseline, changing along with sleep states. This study explores automatic sleep stage classification using different physiological signals, including six-channel EEG, EOG-L, EOG-R, and Chin a-b signals. The PCBSleepNet model is applied to conduct sleep staging experiments using these signals, all sampled at 200 Hz. The experimental results are summarized in Table 3, it can be seen that the six-channel EEG achieved the best performance. Among the single-channel signals, the EOG-L channel demonstrated notable performance within the PCBSleepNet model, achieving an overall accuracy of 82.4%, a Kappa coefficient of 0.71, and an MF1 score of 78.9%. The EOG-R channel also achieved a performance similar to EOG-L, with results comparable to single-channel EEG signals. However, the Chin a-b EMG channel exhibited relatively weaker performance in comparison.

Table 3 Experimental Results of Automatic Sleep Stage Classification Using Different Physiological Signals

Physiological Signals	Acc (%)	Kappa	MF1 (%)
Six-channal EEG	89.4	0.85	85.2
EOG-L	82.4	0.71	78.9
EOG-R	81.6	0.70	76.3
Chin a-b	74.8	0.64	69.6

3.3 Multimodal Study on Different Physiological Signals

Building upon the previous research, this section explores a multimodal approach by integrating different physiological signals from the PSG dataset. The C3-M2 EEG channel, which demonstrated superior sleep staging performance in SMHCSD, was selected as the primary input signal. It was combined with the EOG-L channel from EOG signals and the Chin a-b EMG signal to form a multi-physiological input for training the PCBSleepNet model. The final experimental results were analyzed based on these multimodal inputs. As observed from the data in Table 4, combining EEG signals with other physiological signals resulted in improved model performance compared to using the C3-M2 EEG channel alone. The EEG+EOG+EMG combination achieved the best results, with an overall accuracy of 89.5%, a Kappa coefficient of 0.85, and an MF1 score of 85.5%.

Table 4 Experimental Results of Automatic Sleep Stage Classification Using Different Combinations of Physiological Signals

Combinations of Physiological Signals	Acc (%)	Kappa	MF1 (%)
Six-channal EEG	89.4	0.85	85.2
C3-M2+EOG-L	89.2	0.83	85.3
C3-M2+EMG	89.1	0.83	85.2
C3-M2+EOG-L+EMG	89.5	0.85	85.5

4 DISCUSSION

Building on the single-channel EEG PCBSleepNet model, we extended the evaluation to multi-channel EEG, EOG, EMG, and hybrid signals for sleep staging, while analyzing inter-signal correlations. The feature extraction module utilizes three parallel CNNs with varying kernel sizes to concurrently capture local details and global patterns. An adaptive pooling layer integrates multi-scale features while accommodating input sequence variations. Residual connections with ReLU activations address gradient vanishing while enhancing nonlinear representations. This architecture enables four-layer single-branch networks without performance loss, outperforming traditional stacked 1D-CNNs in convergence. Differentially initialized parallel branches learn complementary features, with output fusion reducing individual branch error impacts. The BiLSTM network outperforms traditional RNNs through bidirectional temporal processing. Its bidirectional architecture captures temporal dependencies in both directions, improving contextual awareness. Gated mechanisms model sleep stage transitions while mitigating RNNs' gradient vanishing issues. Despite higher computational costs, BiLSTM's accuracy gains justify its clinical implementation potential.

This study evaluates EEG channel selection effects through systematic performance comparisons. Six-channel EEG achieved superior performance (vs. single/dual channels), demonstrating multi-channel integration enhances feature richness and model robustness. Optimal single/dual channels (C3-M2, C4-M1+C3-M2) benefit from central scalp coverage capturing critical sleep features through sensorimotor activity monitoring. Occipital combinations (O2-M1+O1-M2) showed reduced efficacy, reflecting their limited sleep-stage relevance. Multi-channel EEG enables comprehensive feature learning across brain regions, optimizing classification. Performance variations underscore channel selection's critical impact, proposing strategic optimization for future studies.

EEG signals maintain superior performance in sleep staging compared to other physiological modalities. EOG signals (EOG-L/R) demonstrate reduced efficacy despite REM stage relevance. EOG primarily monitors eye

movements, contributing mainly to the identification of rapid eye movement (REM) sleep. However, since EOG signals only reflect ocular activity, their feature richness in overall sleep staging is limited, leading to lower classification performance compared to EEG signals. Chin EMG (a-b) shows lowest accuracy due to noise susceptibility and muscle activity specificity. Additionally, EMG signals may vary significantly across individuals, requiring models with strong generalization capabilities to adapt to diverse physiological characteristics. Despite the relatively weak performance of the Chin a-b channel, it still provides valuable auxiliary information for sleep staging, especially in distinguishing REM and non-REM (NREM) sleep. A key feature of REM sleep is a significant reduction in muscle tone, whereas muscle tone remains relatively higher during NREM sleep. This distinction helps reduce false positives and false negatives, avoiding signal redundancy, enhancing signal diversity and differentiation, and ultimately improving the performance of automatic sleep staging models.

Given the outstanding performance of the C3-M2 single-channel EEG signal in sleep staging, as well as the supportive role of other EEG, EOG, and EMG signals, we further compared the performance of the C3-M2 EEG signal combined with different channels of EEG, EOG, and EMG signals. The results demonstrate that EEG signals serve as the core signals for sleep staging, while EOG and EMG signals act as auxiliary signals, further enhancing the classification performance of the model. This indicates that the integration of these signals can provide a more comprehensive representation of physiological changes during sleep. Additionally, the experimental results of different physiological signal combinations appear relatively close. This is because the input data consists of multi-channel data built upon the C3-M2 EEG signal, combined with other physiological signals. The PCBSleepNet model has already achieved strong performance when using the C3-M2 EEG signal alone. By incorporating additional physiological signals, the model receives more training data, helping improve the overall performance of automatic sleep staging. Multi-physiological signals help reduce misclassification in automatic sleep staging because different physiological signals contain both similar and distinct sleep stage features. The waveforms of these signals can complement each other—when features in one signal are unclear, other signals can provide supplementary information, helping the model make more accurate decisions. In multi-modal physiological signal research, integrating EEG signals with other physiological signals (such as EOG and EMG) allows the model to consider multiple sources of information simultaneously, improving its ability to recognize sleep stage transitions. Moreover, multi-physiological signal models can better adapt to individual differences in sleep patterns, as physiological signal characteristics vary among individuals. By leveraging multiple signals, the model can assess sleep stages from multiple perspectives, ultimately improving its robustness and adaptability.

Furthermore, our dataset derived from the Shanghai Mental Health Center holds particular clinical relevance, as it represents sleep characteristics of Asian populations. Current sleep staging research predominantly relies on European/American datasets, while potential cross-cultural differences in sleep architecture due to sociocultural and socioeconomic factors[26] remain understudied. This dataset may provide crucial evidence for developing sleep health interventions tailored to Asian demographics. Notwithstanding these advancements, this study has limitations. The model's performance remains constrained by the relatively limited scale of our dataset, a common challenge in deep learning applications requiring substantial training data. Future work should focus on expanding dataset size through multicenter collaborations and optimizing network architecture to enhance generalizability and overall performance.

5 CONCLUSIONS

This study advances automated sleep staging research by leveraging multi-physiological signals recorded by polysomnography (PSG) within the PCBSleepNet framework. We confirmed the central role of EEG signals in sleep staging while demonstrating the significant performance enhancement achievable through auxiliary EOG and EMG signals.

COMPETING INTERESTS

The authors have no relevant financial or non-financial interests to disclose.

REFERENCES

- [1] Smith M G, Witte M, Rocha S, et al. Effectiveness of incentives and follow-up on increasing survey response rates and participation in field studies. *BMC Medical Research Methodology*, 2019, 19(1).
- [2] Phan H, Andreotti F, Cooray N, et al. Joint Classification and Prediction CNN Framework for Automatic Sleep Stage Classification. *IEEE Transactions on Biomedical Engineering*, 2019, 66(5): 1285-1296.
- [3] Czeisler C A. Duration, timing and quality of sleep are each vital for health, performance and safety. *Sleep Health: Journal of the National Sleep Foundation*, 2015, 1(1): 5-8.
- [4] Korkalainen H, Aakko J, Nikkonen S, et al. Accurate Deep Learning-Based Sleep Staging in a Clinical Population With Suspected Obstructive Sleep Apnea. *IEEE Journal of Biomedical and Health Informatics*, 2020, 24(7): 2073-2081.
- [5] Rundo J V, Downey R. Chapter 25 - Polysomnography. In: Levin K H, Chauvel P (Eds.), *Handbook of Clinical Neurology*, Elsevier, 2019: 381-392.

- [6] Berry R B, Brooks R, Gamaldo C, et al. AASM Scoring Manual Updates for 2017 (Version 2.4). *Journal of Clinical Sleep Medicine*, 2017, 13(5): 665-666.
- [7] Silber M H, Ancoli-Israel S, Bonnet M H, et al. The Visual Scoring of Sleep in Adults. *Journal of Clinical Sleep Medicine*, 2007, 3(2): 121-131.
- [8] Chapotot F, Becq G. Automated sleep-wake staging combining robust feature extraction, artificial neural network classification, and flexible decision rules. *International Journal of Adaptive Control and Signal Processing*, 2010, 24(5): 409-423.
- [9] Allan Hobson J. A manual of standardized terminology, techniques and scoring system for sleep stages of human subjects: A. Rechtschaffen and A. Kales (Editors). *Electroencephalography and Clinical Neurophysiology*, 1969, 26(6): 644.
- [10] Rosenberg R S, Hout S V. The American Academy of Sleep Medicine Inter-scorer Reliability Program: Respiratory Events. *Journal of Clinical Sleep Medicine*, 2014, 10(4): 447-454.
- [11] Grigg-Damberger M M. The AASM scoring manual: a critical appraisal. *Current Opinion in Pulmonary Medicine*, 2009, 15(6).
- [12] Zhang L, Fabbri D, Upender R, et al. Automated sleep stage scoring of the Sleep Heart Health Study using deep neural networks. *Sleep*, 2019, 42(11).
- [13] Ben Hamouda G, Rejeb L, Ben Said L. Ensemble learning for multi-channel sleep stage classification. *Biomedical Signal Processing and Control*, 2024, 93: 106184.
- [14] Heng X, Wang M, Wang Z, et al. Leveraging discriminative features for automatic sleep stage classification based on raw single-channel EEG. *Biomedical Signal Processing and Control*, 2024, 88: 105631.
- [15] Fu G, Zhou Y, Gong P, et al. A Temporal-Spectral Fused and Attention-Based Deep Model for Automatic Sleep Staging. *IEEE Transactions on Neural Systems and Rehabilitation Engineering*, 2023, 31: 1008-1018.
- [16] Jiang D, Ma Y, Wang Y. Sleep stage classification using covariance features of multi-channel physiological signals on Riemannian manifolds. *Computer Methods and Programs in Biomedicine*, 2019, 178: 19-30.
- [17] Wang X, Bik A, de Groot E R, et al. Feasibility of automated early postnatal sleep staging in extremely and very preterm neonates using dual-channel EEG. *Clinical Neurophysiology*, 2023, 146: 55-64.
- [18] Satapathy S K, Bhoi A K, Loganathan D, et al. Machine learning with ensemble stacking model for automated sleep staging using dual-channel EEG signal. *Biomedical Signal Processing and Control*, 2021, 69: 102898.
- [19] Sokolovsky M, Guerrero F, Paisarnrisomsuk S, et al. Deep Learning for Automated Feature Discovery and Classification of Sleep Stages. *IEEE/ACM Transactions on Computational Biology and Bioinformatics*, 2020, 17(6): 1835-1845.
- [20] Zhuang L, Dai M, Zhou Y, et al. Intelligent automatic sleep staging model based on CNN and LSTM. *Frontiers in Public Health*, 2022, 10.
- [21] Fiorillo L, Favaro P, Faraci F D. DeepSleepNet-Lite: A Simplified Automatic Sleep Stage Scoring Model With Uncertainty Estimates. *IEEE Transactions on Neural Systems and Rehabilitation Engineering*, 2021, 29: 2076-2085.
- [22] Haowei Z, Zhe X, Chengmei Y, et al. Automatic sleep staging model based on single channel electroencephalogram signal. *Journal of Biomedical Engineering*, 2023, 40(3): 458-464+473.
- [23] Yang Y, Li S, Li C, et al. Research on ultrasonic signal processing algorithm based on CEEMDAN joint wavelet packet thresholding. *Measurement*, 2022, 201: 111751.
- [24] He H B, Bai Y, Garcia E A, et al. ADASYN: Adaptive Synthetic Sampling Approach for Imbalanced Learning. 2008 IEEE International Joint Conference on Neural Networks, 2008: 1322-1328.
- [25] Michielli N, Acharya U R, Molinari F. Cascaded LSTM recurrent neural network for automated sleep stage classification using single-channel EEG signals. *Computers in Biology and Medicine*, 2019, 106: 71-81.
- [26] Willoughby A R, Alikhani I, Karsikas M, et al. Country differences in nocturnal sleep variability: Observations from a large-scale, long-term sleep wearable study. *Sleep Medicine*, 2023, 110: 155-165.